The Structure of Aluminosilicate Glasses: High-Resolution ^{17}O and ^{27}Al MAS and 3QMAS NMR Study

Sung Keun Lee* **and Jonathan F. Stebbins**

Department of Geological and Environmental Sciences, Stanford University, Stanford, California 94305

Received: December 6, 1999; In Final Form: February 15, 2000

We investigate short-range order and local atomic configuration in charge-balanced aluminosilicate glasses as functions of composition, using ^{17}O and ^{27}Al MAS and triple-quantum magic angle spinning (3QMAS) NMR spectroscopy. Enhanced resolution in ^{17}O and ^{27}Al 3QMAS spectra, compared to MAS NMR, allows the quantification of the spectra and the extent of disorder using a semiempirical function relating 3QMAS efficiency to a quadrupolar coupling constant (C_q). The variations with the Si/Al ratio (R) in peak positions and widths in the isotropic dimension of ^{27}Al 3QMAS NMR spectra in both Na- and Ca-aluminosilicate glasses can be ascribed to variations in the populations of Al sites with varying numbers of Al vs Si neighbors with composition. In the ^{17}O 3QMAS spectra, variations of populations of three clearly resolved oxygen sites (Al−O−Al, Si−O−Al, and Si−O−Si) with R and cation field strength are consistent with the predictions given in our previous results from ^{29}Si MAS NMR. The quadrupolar coupling product (P_q) of each oxygen site does not vary significantly with R, but it increases with cation field strength. On the other hand, isotropic chemical shifts (δ_{iso}^{CS}) increase with decreasing R and increasing cation field strength. These trends suggest that the configuration and framework connectivity in aluminosilicate glasses and melts are relatively constant with R but can be perturbed by high field strength cations with increased Al−O−Al and angular disorder, manifested by the increased variation of δ_{iso}^{CS} and the formation of non-bridging oxygen (NBO). The extent of disorder in aluminosilicate glasses is reflected in calculated configurational enthalpy, which increases with increasing cation field strength, consistent with the excess enthalpy of mixing data from calorimetry. The method and results given here provide improved prospects for the quantitative application of 3QMAS NMR and add to a more complete understanding of framework site connectivity in aluminosilicate glasses.

Introduction

Aluminosilicate glasses and liquids have long been studied not only because of their applications in the glass and ceramics industries but also because of their relevance to the properties of natural magmas.[1−10] Solid state NMR, particularly ^{29}Si magic angle spinning (MAS) NMR, has been one of the important tools for investigating atomic configurations and, thus, the relationship between macroscopic properties and local structure of these materials.[8,11−13] However, in such glasses, unresolved ^{29}Si MAS NMR spectra often impart difficulties in data analysis, making this method rather model dependent.[8] On the other hand, recent studies of quadrupolar nuclides, such as ^{17}O, using triple-quantum MAS (3QMAS) NMR show enhanced resolution, free from quadrupolar broadening in the so-called "isotropic dimension" and have presented new experimental findings, such as the existence of non-bridging oxygen (NBO) and Al−O−Al linkages in charge-balanced Ca- and Na-aluminosilicates (e.g. glasses on the $Ca_{0.5}AlO_2-SiO_2$ and $NaAlO_2-SiO_2$ joins).[14,15] These results have suggested that conventional views of structural disorder, in which Al and Si tetrahedra are fully polymerized and Al−O−Al linkages are absent ("Al avoidance"), are not the strict rules controlling short-range order but may be only first approximations, especially for systems containing higher charged cations (e.g., Ca^{2+} vs Na^+).

Framework cation distribution is one of the major controls on the configurational thermodynamic properties in aluminosilicate glasses.[8,16−18] The effect of the charge-balancing cation on the extent of deviation from perfect Al avoidance was recently quantified by detailed ^{29}Si studies and modelings of glasses in the $NaAlO_2-SiO_2$ and $Ca_{0.5}AlO_2-SiO_2$ systems.[8,15,19] These studies allowed the prediction of the distributions of Si sites with varying numbers of Al next nearest neighbors and vice versa, as well as the variation of oxygen site populations with respect to Si/Al ratio (R) and cation field strength. It could be important to confirm and extend these studies by directly investigating the local Al and O environment with ^{27}Al and ^{17}O NMR. However, despite its extensive usefulness for the structural analysis of aluminosilicate glasses and crystals,[6,7,20,21] 3QMAS technique is generally not quantitative. Accurate spin populations of each structural site cannot always be obtained directly from normal 3QMAS spectra because the peak intensities decrease with increasing quadrupolar coupling constant (C_q).[22−25] Therefore, it would be useful to have a simple analytical expression for the dependence of 3QMAS efficiency on C_q that can be used to scale experimental 3QMAS intensities and to obtain the true site populations.[26]

In this study, we present ^{17}O and ^{27}Al MAS and 3QMAS NMR spectra of aluminosilicate glasses with varying R and cation field strength, including $NaAlSiO_4$ and $LiAlSiO_4$ glasses, which are the best candidates for studying the inherent disorder in aluminosilicates on charge-balanced joins.[8] $LiAlSiO_4$ glasses are also important for high-temperature glass ceramics because of their low thermal expansivity.[27,28] We quantify the extent of disorder of framework cations (Si and Al) from the site populations of quadrupolar nuclei obtained from ^{27}Al and ^{17}O 3QMAS NMR spectra scaled using a semiempirical analytical

10.1021/jp994273w CCC: $19.00
Published on Web 04/07/2000

expression for MQMAS efficiency. Finally, we discuss the short-range and intermediate-range atomic structure of aluminosilicate glasses in general.

A summary of the NMR parameters mentioned in this study is given below. δ_{3qmas} is the peak position in the isotropic dimension in 3QMAS NMR spectra. δ_{iso}^{CS} is the true isotropic chemical shift, which is free from quadrupolar interaction. C_q is the quadrupolar coupling constant, e^2qQ/h, where eQ and eq are the quadrupolar moment and the principle component of the electric field gradient, respectively, at the site of interest. P_q is the quadrupolar coupling product, $C_q(1 + \eta^2/3)^{1/2}$, where η is the asymmetry parameter. δ_{iso}^{2Q} is the second-order quadrupolar shift for spin-$^5/_2$ nuclei, $6000P_q^2/\omega_0^2$ where ω_0 is the Larmor frequency.

For a spin-$^5/_2$ nuclei such as ^{27}Al and ^{17}O, the observed resonance frequency in the isotropic dimension (ω_1) of 3QMAS spectrum is given by

$$\delta_{3QMAS} = -17/31\delta_{iso}^{CS} + 10/31\delta_{iso}^{2Q} \quad (1)$$

The center of gravity of same peak in the MAS dimension (ω_2) is

$$\delta_{3QMAS} = \delta_{iso}^{CS} + \delta_{iso}^{2Q} \quad (2)$$

From the above relations, at least mean values of P_q and δ_{iso}^{CS} of each oxygen site can be estimated. Because of the small difference between P_q and C_q in these systems ($\sim$4% for $\eta = 0.5$), we assume that $P_q \approx C_q$.

Experimental Methods

Sample Preparation. The glasses were synthesized as described previously[8] from ^{17}O-enriched SiO_2 and Al_2O_3, Na_2CO_3, Li_2CO_3, and $CaCO_3$ reagents with about 0.2 wt % Co_3O_4, which was added to speed the spin lattice relaxation. The mixtures were decarbonated at 750 °C and then fused at 1600 °C for 1 h under argon. The resulting glasses, except $LiAlSiO_4$, were analyzed by electron microprobe and appeared to be homogeneous and close to nominal compositions.[8] The sample preparation for $R = 0.7$ and $R = 3$ glasses was reported previously.[7,19] Natural kyanite (Al_2SiO_5, SU# 24861, locality: Brazil), which has four sites with equal populations, with C_q's of 3.7, 6.5, 9, and 10 MHz, respectively,[29] was studied in order to estimate the C_q dependence of the 3QMAS efficiency.

NMR Spectroscopy. NMR experiments were done with a modified Varian VXR-400S spectrometer at a Larmor frequency of 54.22 and 104.219 MHz for ^{17}O and ^{27}Al, respectively. In ^{17}O MAS NMR experiments, powdered samples were packed into 5 mm silicon nitride rotors and spun at 14 kHz in a Doty Scientific MAS probe. The Peak positions are reported relative to external tap water. Recycle delays of 1 s were used with a radio frequency pulse length of 0.4 μs, which is about a 15° tip angle for the central transition in solids. A constant Gaussian apodization was applied to increase signal-to-noise ratios but was adjusted to ensure that the final peak widths did not exceed those of unapodized data by more than 0.3 ppm. ^{17}O 3QMAS spectra were obtained using the shifted-echo pulse sequence consisting of two hard (ideally nonselective) pulses and a soft, selective pulse.[6,30] The spin−lattice relaxation time for each sample was measured with the saturation-recovery method, and the delay times were chosen to be $3 \times T_1$, which was typically 1 to 2 s. The optimized first and second pulse durations were 5.25 and 1.75 μs, respectively; the final π pulse had a duration of 24 μs. The delay time between the second pulse and the third pulse was an integer multiple of the rotor period, about 1 ms. Typically, about 68 t_1 increments were necessary for a spectral width of 50 kHz. For a signal-to-noise ratio sufficient to observe even signals with relatively low intensity, 1534 scans per increment were used for the $R = 1$ and $R = 3$ sodium aluminosilicate glasses and $LiAlSiO_4$ glasses, and 834 scans per increment were used for the $R = 0.7$ glass. Only the echo part of the data set was used in processing the resulting 2-dimensional spectra.[7]

For ^{27}Al MAS and 3QMAS experiments, the spinning rate was 14.6 kHz, and peak positions were reported relative to external 1 M aqueous $Al(NO_3)_3$. In MAS experiments, the recycle delays were 1 s, and the radio frequency pulse length was 0.4 μs. A constant Gaussian apodization was applied allowing less than 0.3 ppm difference in peak widths, compared with the unapodized spectra. ^{27}Al 3QMAS spectra were obtained using the shifted-echo pulse sequence.[6,30] The first and second 2π pulses were each 4.5 μs long. A soft π pulse, which was central-transition selective, was about 19 μs long. ^{27}Al 3QMAS NMR spectra for glasses and for kyanite were obtained under the same experimental conditions. Both the echo and the anti-echo part were used in processing, with the exception of kyanite, in which only the echo part was used, ^{27}Al 3QMAS data was used.

Fitting Procedures for ^{27}Al 3QMAS NMR Spectra of Glass. Here, the total projections in the isotropic dimension of the ^{27}Al 3QMAS spectra of the Na-aluminosilicate glasses were decomposed into several subpeaks representing the five possible Al species with 0−4 Si next nearest neighbors [$Q^4(n\text{Si})$]. The population of each site was obtained from the degree of Al avoidance (Q), taken from our previous results, in which $Q = 1$ refers to perfect obedience of the Al avoidance rule, and $Q = 0$ represents a fully random distribution of Si and Al ($0.93 \leq Q \leq 0.99$ for Na-aluminosilicate glasses).[8,15] The Al site populations were adjusted for fitting using the scaling function of 3QMAS efficiency (see below), which leads to the decrease in $Q^4(3\text{Si})/Q^4(4\text{Si})$ in $R = 1$ glasses from 0.96 to 0.70 at $Q = 0.94$. All of the spectra for a series of glasses were fitted *simultaneously* by a nonlinear least-squares algorithm with the adjusted site populations as areas of Gaussian-shaped peaks. The only adjustable parameters are five peak widths and five peak positions.[8] Because the chemical shifts in crystalline model compounds have been reported only for $Q^4(4\text{Si})$ and $Q^4(0\text{Si})$, the results are not unique, but the obtained systematic trend of variation of peak positions and widths suggests that those fitting results are valid and represent the population variation of each $Q^4(n\text{Si})$ (see the Results).

Theory

Dependence of 3QMAS Efficiency on C_q. As mentioned above, signal intensities in 3QMAS spectra do not necessarily represent the accurate site populations. On the other hand, the 3QMAS technique can be quantitative in crystals for cases in which the quadrupolar parameters (C_q and η) obtained from this technique are used for fitting single pulse MAS spectra, from which the population of each structural unit can be obtained.[22] However, this approach may be difficult for glasses with distributions of those parameters.

The dependency of 3Q excitation and −1Q conversion on C_q in the 3QMAS experiment, as obtained from numerical or analytical analysis, can, conversely, be utilized to quantify the spectra, provided that other parameters, such as radio frequency field strength, ω_1, and pulse lengths are known. The correlations between C_q and 3QMAS populations have been derived

analytically[22,26,31] and numerically[23,25,32] by considering the time evolution of the spin-density matrix. On the other hand, the exact and experiment-specific dependence on C_q of MQMAS efficiency can also be obtained from the experiment using the crystals with well-known site populations and C_q's.[30]

Here, the theoretical procedures of obtaining the scaling function of 3QMAS efficiency with respect to C_q, and other experimental conditions for a single crystal with spin-$^3/_2$ are presented. Given the approximations and assumptions, the purpose of this derivation is not to obtain the exact solution that matches the experiment but, rather, to obtain the approximate functional form of the scaling function that can then be used with experimental calibrations.

The spin Hamiltonian (H) for a spin-$^3/_2$ nuclei in the rotating frame, considering only 1st order quadrupolar interaction, is given below as[33]

$$H = \frac{\upsilon_q}{2}(3\cos^2\theta - 1 - \eta\sin^2\theta\cos 2\varphi)(3S_z^2 - S(S+1)) + \upsilon_1 S_x \quad (3)$$

where S_z and S_x are spin angular momentum operator and S is and spin quantum number. The variable υ_q is the quadrupolar frequency defined as

$$\upsilon_q = \frac{e^2qQ}{2S(2S-1)h} \quad (4)$$

θ and φ define the orientation of the external magnetic field in the principal axis system of the electric field gradient tensor. The radio frequency field strength is υ_1 (Hz). The 3QMAS efficiency can be obtained from the time evolution of the spin-density matrix by solving the Liouville−von Neumann equation

$$\frac{d}{dt}\rho(t) = -i[H(t),\rho(t)] \quad (5)$$

The solution in the rotating frame can be expressed as

$$\rho(t) = e^{-iHt}\,\rho(0)e^{iHt} \quad (6)$$

The analytical solution of eq 6 in the spin-$^3/_2$ system has been obtained using a fictitious spin-$^1/_2$ Hamiltonian formalism in which each operator $(I_{ij}^p)_{p=x,y,z}$, describes a transition between two energy levels i and j,[22,26,31] and the Hamiltonian given in eq 3 can be written as[31]

$$H = \upsilon_q(I_z^{12} - I_z^{34}) - \sqrt{3}\upsilon_1(I_x^{12} + I_x^{34}) - 2\upsilon_1 I_x^{23} \quad (7)$$

where 1, 2, 3, and 4 denote the eigen states of S_z from $m_z = {}^3/_2$ to $-{}^3/_2$.

3Q coherence evolved under H can be generated after the excitation by a single pulse with length "t" and can be obtained by solving eq 6 assuming an equilibrated density matrix of $\rho(0) \propto I_z^{23} + 3I_z^{14}$. Its efficiency $< I_y^{14} >$ is proportional to its coefficient, a_y^{14}. Assuming that $\upsilon_1 \ll \upsilon_q$, a_y^{14} may be written as

$$a_y^{14}(t) \propto \sin[(\upsilon_1 + {}^1/_2(\upsilon^{13} + \upsilon^{24}))2\pi\, t] \quad (8)$$

where $\upsilon^{13} = (3\upsilon_1^2 + (\upsilon_q - \upsilon_1)^2)^{1/2}$ and $\upsilon^{24} = -(3\upsilon_1^2 + (\upsilon_q + \upsilon_1)^2)^{1/2}$.

After the conversion of triple-quantum into single-quantum observables, assuming I_x^{14} as the initial spin-density matrix under RF-pulse of length t_1, the final state consists of single quantum coherence, I_x^{23}, whose coefficient a_x^{23} is proportional to the conversion efficiency and can be expressed, again assuming $\upsilon_1 \ll \upsilon_q$, as[22,26,31]

$$a_x^{23}(t_1) \propto \sin^2\theta'(2 - \cos 2\pi\upsilon^{13}t_1 - \cos 2\pi\upsilon^{24}t_1) \quad (9)$$

where $\theta' = \tan^{-1}(\sqrt{3}\upsilon_1/\upsilon_q)$

More general expressions for eqs 8 and 9 have been reported.[26,31] The final signal intensity may be expressed as

$$F(t,t_1,\upsilon_1,\upsilon_q) \propto \sin\left[\left(\upsilon_1 + \frac{1}{2}(\upsilon^{13} + \upsilon^{24})\right)2\pi\, t\right]\sin^2\theta'(2 - \cos 2\pi\upsilon^{13}t_1 - \cos 2\pi\upsilon^{24}t_1) \quad (10)$$

The 3QMAS efficiency decreases with increasing C_q and may be used as a scaling function to obtain the accurate relative site populations among different structural sites, i.e.,

$$I^a/I^b = (A^aF(C_q{}^b))/(F(C_q{}^a)A^b) \quad (11)$$

where I^i are the 3QMAS signal intensities in the isotropic projection, and A^i are true spin populations of sites a and b with quadrupolar coupling constants C_q^a and C_q^b. As illustrated in Figure 1, $F(C_q)$ is a decaying function of C_q and can be simply approximated using a Gaussian function

$$F(C_q) \propto \exp(-(C_q)^2/2\sigma^2) \quad (12)$$

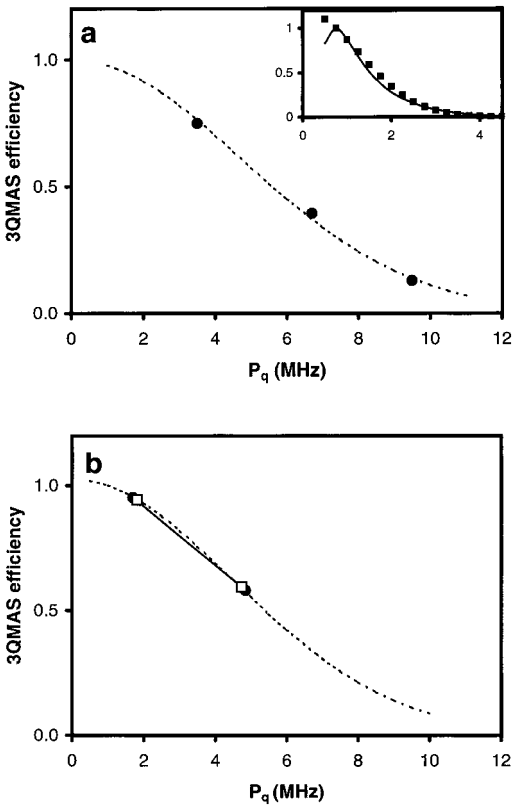

Figure 1. Experimental dependence of 3QMAS efficiency on C_q for Al sites in kyanite (a) and for oxygen sites in $NaAlSiO_4$ and $LiAlSiO_4$ glasses (b). Closed circles represent the experimental intensity of each site in kyanite (a) and $NaAlSiO_4$ (b). Open squares are the experimental intensities for $LiAlSiO_4$ glass (b). Dotted lines represent the fitting results using the eq 12 with $\sigma = 4.7$ and 4.5 for kyanite (Al_2SiO_5) and aluminosilicate glasses, respectively. Solid line in inset denotes the 3QMAS efficiency calculated from eq 10 for spin-$^3/_2$ nuclei in single crystal. RF field strength is 100 kHz and $\upsilon_1 t$ (3Q excitation) and $\upsilon_1 t_1$ (-1Q conversion) are 0.8 and 0.1 (cycle), respectively. Closed squares are fitting results using eq 12.

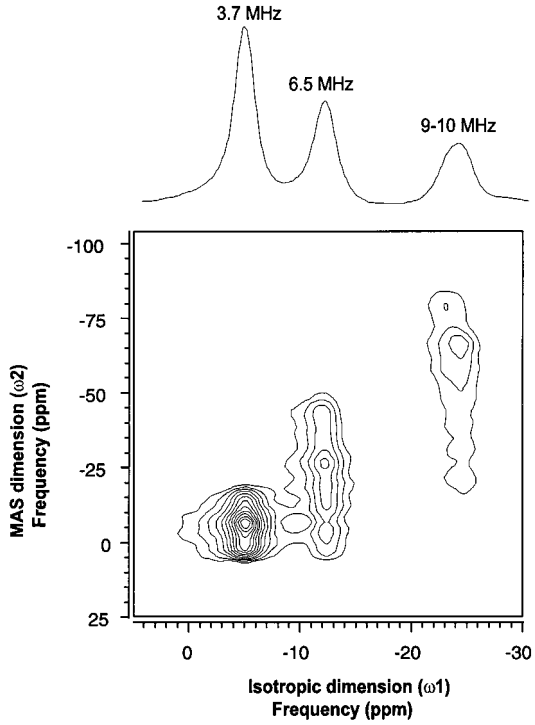

Figure 2. ^{27}Al 3QMAS NMR spectra of kyanite (Al_2SiO_5). The total projection in the isotropic dimension is shown above the 2-dimensional plot, with known C_q values.

where σ is a constant that depends on the experimental conditions, such as pulse lengths (t, t_1) and RF field strength (υ_1), and the σ value can be obtained by fitting results from specific experiments on crystals or glasses for which the site populations and C_q's are well-known. For spin-$^5/_2$ nuclides, a similar trend, in which 3QMAS efficiency decays with increasing C_q, can be expected, as shown in the numerical calculations.[32] To obtain σ for our ^{27}Al 3QMAS experiment, we recorded the 3QMAS spectrum of kyanite (Figure 2).[30,34] Figure 1a shows the fitting results of 3QMAS efficiency with respect to C_q using eq 12, which leads to a value for σ of about 4.7 for a C_q range from about 3 to 10 MHz with the experimental conditions given above. For our ^{17}O 3QMAS experiment, we can obtain σ from the fact that true site population of Si−O−Si and Al−O−Al in $R = 1$ aluminosilicate glasses should be equal, which leads to a value of σ of about 4.5 for a C_q range from 1.5 to 5 MHz.

Calculation of Oxygen and Aluminum Site Populations. The oxygen site populations in charge-balanced aluminosilicate glasses were derived as a function of temperature, order parameter (degree of Al avoidance, Q), and composition (Si/Al) based on the quasi-chemical approximation.[8] The proportions of Al−O−Al linkages in the aluminosilicate glasses along the $NaAlO_2$−SiO_2 and $Ca_{0.5}AlO_2$−SiO_2 joins can be given as

$$X_{\mathrm{Al-O-Al}} = X_{\mathrm{Al}}\left(1 - \frac{2X_{\mathrm{Si}}}{\beta + 1}\right) \tag{13}$$

where $\beta = \sqrt{1+4X_{\mathrm{Si}}X_{\mathrm{Al}}(\exp(2W/zkT)-1)}$ and X_{Si} and X_{Al} are mole fractions of Si and Al in tetrahedral sites. W is the lattice energy difference of the reaction (Si−O−Si) + (Al−O−Al) = 2(Al−O−Si). The variables z and k are the numbers of tetrahedral neighbors (4 for fully polymerized aluminosilicate) and Boltzman constant, respectively. For sodium aluminosilicates, the obtained degree of Al-avoidance based on the ^{29}Si NMR data ranges from 0.93 to 0.99 and the expected concentrations of Al−O−Al linkages in $NaAlSiO_4$ glass ranges from 5 to 10%.

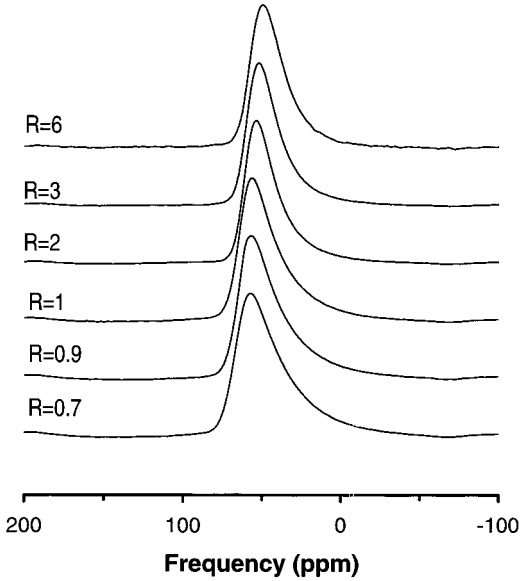

Figure 3. ^{27}Al MAS NMR spectra of sodium aluminosilicate glasses with variable ratios (R) of Si/Al.

Aluminum site populations [Q^4(nSi)] also can be obtained using similar procedures.[8] The probability of finding Si around Al ($P_{\mathrm{Al-Si}}$) can be written as

$$P_{\mathrm{Al-Si}} = X_{\mathrm{Si}}\frac{2}{(\beta + 1)} \tag{14}$$

The proportions of each Q^4(nSi) can be obtained using the binomial distribution and

$$P(n) = {}_4C_n\frac{(2R)^n(R\beta - R + \beta + 1)^{4-n}}{(R\beta + R + \beta + 1)^4} \tag{15}$$

where n is the number of Si around Al as a next nearest neighbor.

Results for Glasses

Sodium Aluminosilicate. Figure 3 shows the ^{27}Al MAS NMR spectra of a series of sodium aluminosilicate glasses with varying R. The peaks are broadened by second-order quadrupolar interaction and shift slightly to lower frequency with increasing R. This kind of MAS NMR line shape, with long "tails" to lower frequency, is typical for distributions of C_q and $\delta_{\mathrm{iso}}^{\mathrm{CS}}$, which is to be expected in glasses.[35] These characteristics hamper quantitative analysis using decomposition into subpeaks representing distinct Al environments. The widths of the spectra can, however, be qualitatively correlated with the number of Q species in the system and increases with decreasing R, suggesting that the number of distinct Al species with significant concentrations increases. Figure 4 shows the ^{27}Al 3QMAS NMR spectra of the same glass series. Only 4-coordinated Al is observed with a detection limit of 2%. The isotropic projections 2−3% clearly indicate that the population of Al sites with smaller $\delta_{3\mathrm{qmas}}$, and hence larger $\delta_{\mathrm{iso}}^{\mathrm{CS}}$, decreases with increasing R, which can be ascribed to a decrease in the fraction of species with fewer than four Si neighbors. There is also a systematic decrease of peak width in the MAS dimension with increasing R, suggesting a decrease in the concentrations of species with larger C_q values (Figure 3). The fitting results of the isotropic

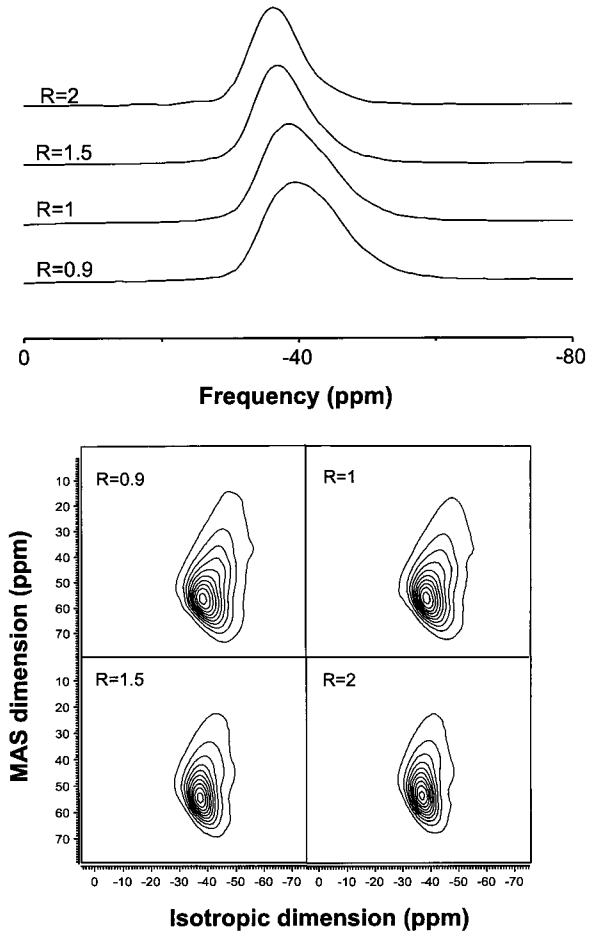

Figure 4. ^{27}Al 3QMAS NMR spectra of sodium aluminosilicate glasses with variable ratios (R) of Si/Al. Total projection in the isotropic dimension is shown above the two-dimensional plot. 10 contour levels are drawn from 7 to 97% of maximum intensity.

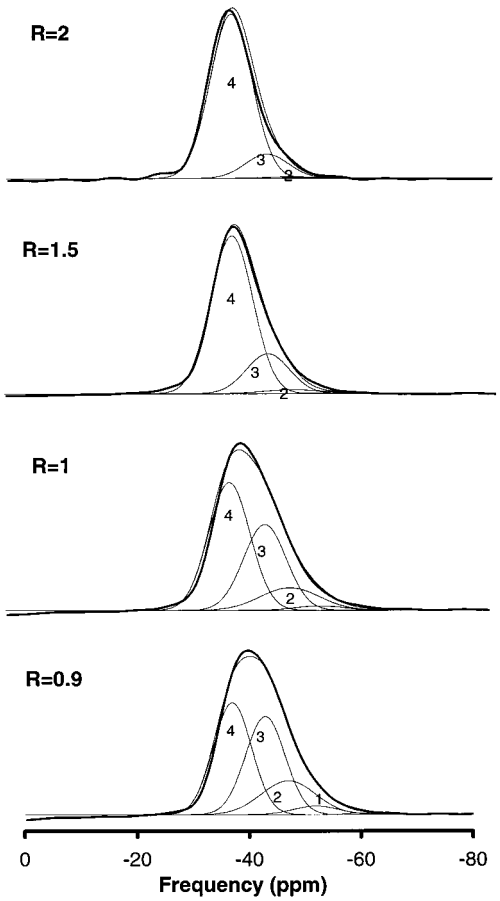

Figure 5. Fitting results for isotropic projection of ^{27}Al 3QMAS NMR spectra of sodium aluminosilicate glasses with a degree of Al avoidance (Q) of 0.94. Thick solids lines are the experimental spectra and thin solid lines show the fitted curves and each component. Numbers of Si next nearest neighbors of each $Q^4(n\text{Si})$ sites are shown.

projections of 3QMAS spectra using $Q = 0.942$ clearly demonstrate this trend (Figure 5). The average C_q's of Q^4(4Si) and Q^4(0Si) are expected to be less than those of other Q species considering the reduced local symmetry of the latter, and thus, the 3QMAS efficiencies of Q^4(4Si) and Q^4(0Si) are expected to be larger than those of other Al environments. The reported values for C_q in crystalline $CaAl_2O_4$ (Q^4(0Si)) are between 2.5 and 4.3 MHz and δ_{iso}^{CS} ranges from 81.2 to 86.2 ppm.[36] C_q for albite ($NaAlSi_3O_8$) and microcline ($KAlSi_3O_8$) (both Q^4(4Si)) are 3.29 and 3.22 MHz, respectively.[37] The C_q values for other sites with 1,2, or 3 Si next nearest neighbors have not been reported. Here, we assume that the most probable C_q of Q^4(4Si) and Q^4(0Si) sites are 3.5 MHz and that those of others are 5 MHz. The latter assumption is rather arbitrary but is comparable with the P_q values of the corresponding peaks (about 6 MHz) obtained from the centers of gravity in 2-D glass spectra. Using the criteria given in previous sections and these assumptions, isotropic projections of each spectra were fitted. Despite the enhanced population of Q^4(0Si), due to its small C_q, the proportion of this species is negligible, implying that clustering of Al is not probable in the intermediate-range structure. With increasing R, the proportions of Q (3 to 1 Si) decrease, leading to the observed decrease of Al sites with large C_q in the 2-D spectra. The fitting results gave -37 ± 1, -42.8 ± 1.5, -47.0 ± 1, -52.0 ± 1, and -58.0 ± 2 ppm for each $Q^4(n\text{Si})$ species with decreasing number of Si. Because of the overlaps among each component, it is not feasible to independently obtain the C_q values from the slices in the MAS dimension. The fitting is not well-constrained and depends to some degree on the C_q values that are assumed, but the results are completely consistent with the predictions from the modeling of the ^{29}Si MAS NMR data.[8]

The ^{17}O MAS NMR spectra for sodium aluminosilicate and $LiAlSiO_4$ glasses are given in Figure 6. The spectra for samples with $R \leq 1$ do not show any features except slight asymmetry in the lower frequency region with no resolution of signal from distinct oxygen sites. On the other hand, the shoulder at about -10 ppm in the MAS spectrum of $NaAlSi_3O_8$ glass suggests that it could be decomposed into subpeaks from two species with different coupling constants.[7,20]

Figure 7 shows the isotropic projections of these spectra, in which the oxygen sites are clearly resolved. The 2-D ^{17}O 3QMAS spectra have recently been presented.[15] The three types of sites that are observed can be unambiguously assigned to Si−O−Si, Si−O−Al, and Al−O−Al, based on previous studies of crystalline model compounds.[7,14,15,20] The observed systematic variations of peak intensity for each site with respect to R is consistent with the prediction given from ^{29}Si MAS NMR.[8] (Si−O−Al)/(Al−O−Al) increases with increasing R. In the $R = 0.7$ glass, as previously reported,[19] the Al−O−Al and Si−O−Al sites are clearly resolved. The broad peak at around -45 ppm in the 3QMAS dimension is the Si−O−Si site, which was not resolved in our previous spectra because it was of a lower signal-to-noise ratio.[19] Its intensity is underestimated because its C_q (about 4.8 MHz) is larger than those of other sites. The Al−O−Al and Si−O−Al peaks are slightly overlapped in spectra for $R = 0.7$ and 1 glasses because both have

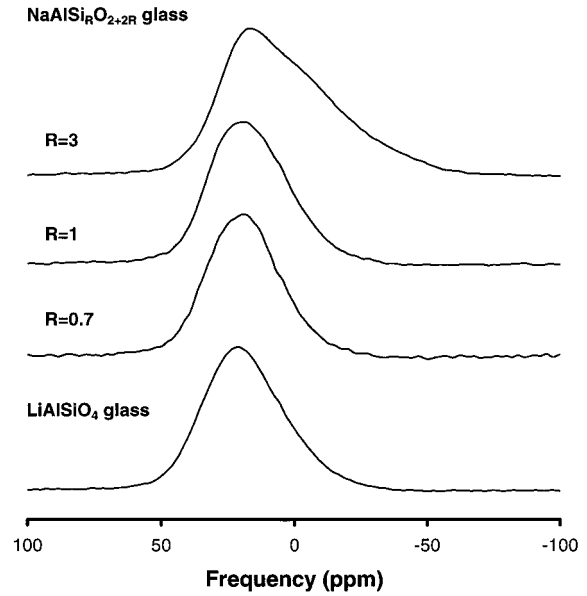

Figure 6. ^{17}O MAS NMR spectra of sodium aluminosilicate glasses with variable ratios (R) of Si/Al, and $LiAlSiO_4$ glass.

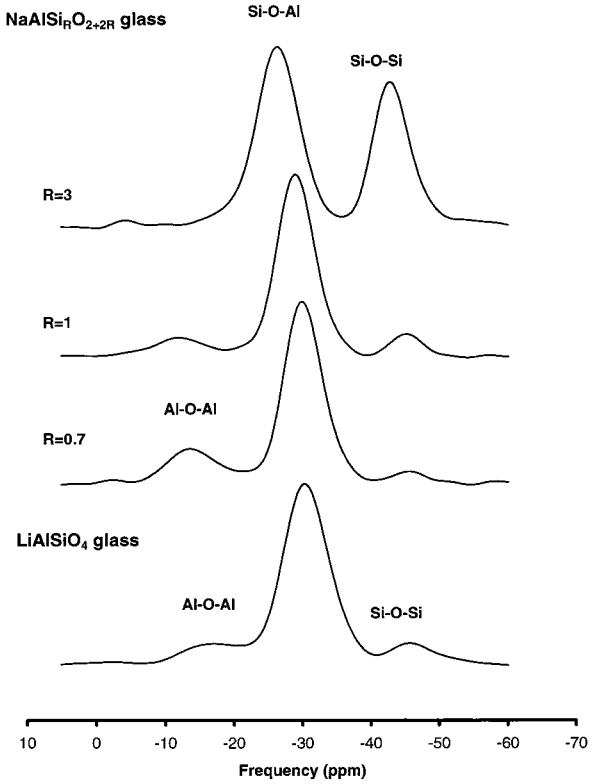

Figure 7. Total projections in the isotropic dimension of ^{17}O 3QMAS NMR spectra for Na-aluminosilicate glasses and $LiAlSiO_4$ glass.

large distributions of δ_{iso}^{CS}, caused by variation in the configurations around the oxygen sites. In $NaAlSiO_4$ ($R = 1$) glass, the Si−O−Si site is more clearly resolved and more intense than that found in the case of $R = 0.7$ spectra because of its higher silica contents.[15] The presence of any Al−O−Al and Si−O−Si at $R = 1$ directly demonstrates that Al avoidance is imperfect. In $NaAlSi_3O_8$ glass, only Al−O−Si and Si−O−Si sites can be resolved.[7,20] However, there is a "tail" on the Al−O−Si peak, which may be related to the wide range of distribution in δ_{iso}^{CS} for this site or, possibly, to a very low concentration of Al−O−Al sites for which the signal intensity is enhanced by a small C_q.

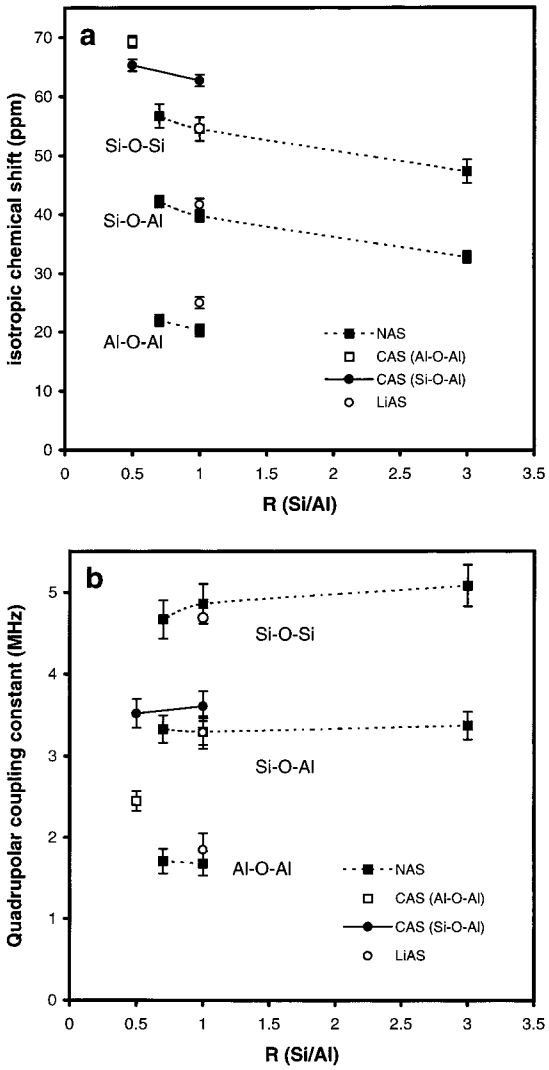

Figure 8. Variation of (a) isotropic chemical shifts and (b) quadrupolar coupling constants in Ca-, Li-, and Na-aluminosilicate glasses with respect to R. Data points for $R = 0.5$ and 1 Ca-aluminosilicate glass are from our previous studies.[14,19]

NMR parameters (P_q and δ_{iso}^{CS}) for each oxygen site were calculated from the positions of the centers of gravity of the peaks in the two dimensions using eqs 1−2 [15] and given in Figure 8. δ_{iso}^{CS} values for all three of the sites decrease systematically with increasing R (Figure 8a), whereas P_q values do not vary greatly (Figure 8b). The P_q value for Al−O−Al of 1.7 MHz is a more accurate determination than that found in our previous report (1.8 MHz).[19] The corrected Al−O−Al population in $NaAlSiO_4$ glass is about 9.5%, which corresponds to a degree of Al-avoidance (Q) of 0.94.[15]

Lithium Aluminosilicate Glasses. The ^{17}O MAS spectrum of $LiAlSiO_4$ glass is again featureless(Figure 6). In contrast, the three types of bridging oxygen sites are clearly resolved in the isotropic projection of the 3QMAS spectrum (Fig. 7). Nonbridging oxygens were not observed, but the signal from such sites may be overlapped with the Si−O−Al peak. The P_q for each site is similar to those in $NaAlSiO_4$ glass. On the other hand, the δ_{iso}^{CS} for Al−O−Al in $LiAlSiO_4$ is slightly higher than that found in $NaAlSiO_4$ glass. Overlap among the peaks increases, compared with $NaAlSiO_4$ glass, because of increased δ_{iso}^{CS} distributions, implying an increase in the number of configurations and, hence, in the disorder, by the introduction of the higher field strength cation(Li^+ vs Na^+). The distribution

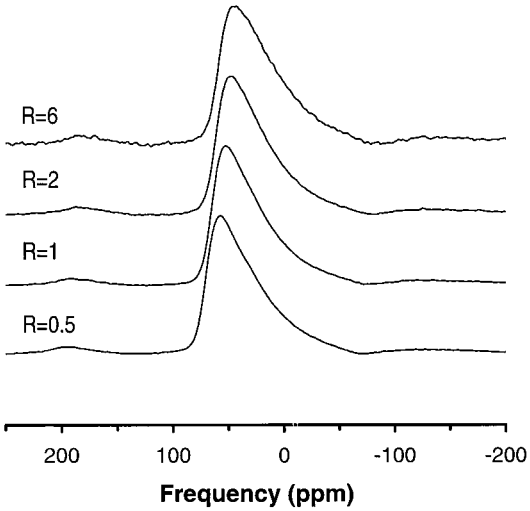

Figure 9. ^{27}Al MAS NMR spectra of calcium aluminosilicate glasses with variable ratios (R) of Si/Al.

of δ_{iso}^{CS} for Al−O−Al is larger than that for Si−O−Si, which also suggests that there are more diverse configurations caused by the arrangement of Li^+ cations near to Al−O−Al sites, perhaps causing a wider bond-angle distribution. The difference in peak positions for Al−O−Al sites between the Na- and Li− aluminosilicate glasses is larger than that for Si−O−Al, suggesting again that the Li^+ cations are more closely associated with Al−O−Al than with Si−O−Al. Using the scaling function given in eq 14, the true populations of Al−O−Al and Si−O−Al sites were estimated to be about 10.6%, corresponding to a degree of Al avoidance at the glass transition temperature of 930 K [38] of about 0.928.[15]

Calcium Aluminosilicate Glasses. Figure 9 shows the ^{27}Al MAS spectra of Ca-aluminosilicate glasses with respect to R. These again show long "tails" toward lower frequencies and do not provide explicit information on the framework cation disorder. ^{27}Al 3QMAS NMR spectra are also not resolved, but the trends in the isotropic projections provide clear evidence of variations of population of Al sites with varying number of Si neighbors, as seen in the Na-aluminosilicate glasses (Figure 10). As Si content increases, the peak positions in the 3QMAS isotropic dimension shift toward higher frequency, accompanied by a shift to lower frequency in the MAS dimension and dominated by a shift to lower frequncy δ_{iso}^{CS}. This trend again suggests that the proportions of $Q^4(n\text{Si})$ with $n < 4$ decrease with increasing R. In contrast to the observed trend, if Al avoidance is complete, there should be no differences in peak positions and shapes for the spectra of glasses with $R \geq 1$ (assuming the same topological disorder), as all of the sites would have four Si neighbors. These qualitative findings are thus consistent with a moderate amount of ordering of framework cations and with the results from ^{29}Si MAS NMR, for which the degree of Al avoidance was found to range from 0.80 to 0.875. Finally, we note that the peak widths in the MAS dimension for the Ca-aluminosilicate glasses are larger than those for Na-aluminosilicate glasses, at least in part due to greater estimated P_q values of about 6.7 MHz.

For ^{17}O, the δ_{iso}^{CS} of Al−O−Si in Ca-aluminosilicate glasses increases with decreasing R from 65.3 ppm ($R = 0.5$) to 62.7 ppm ($R = 1$) as in Na-aluminosilicate glasses (Figure 8).

Discussion

Effect of Composition (Si/Al) on Structure of Aluminosilicate Glasses. NMR parameters, such as δ_{iso}^{CS} and C_q, are

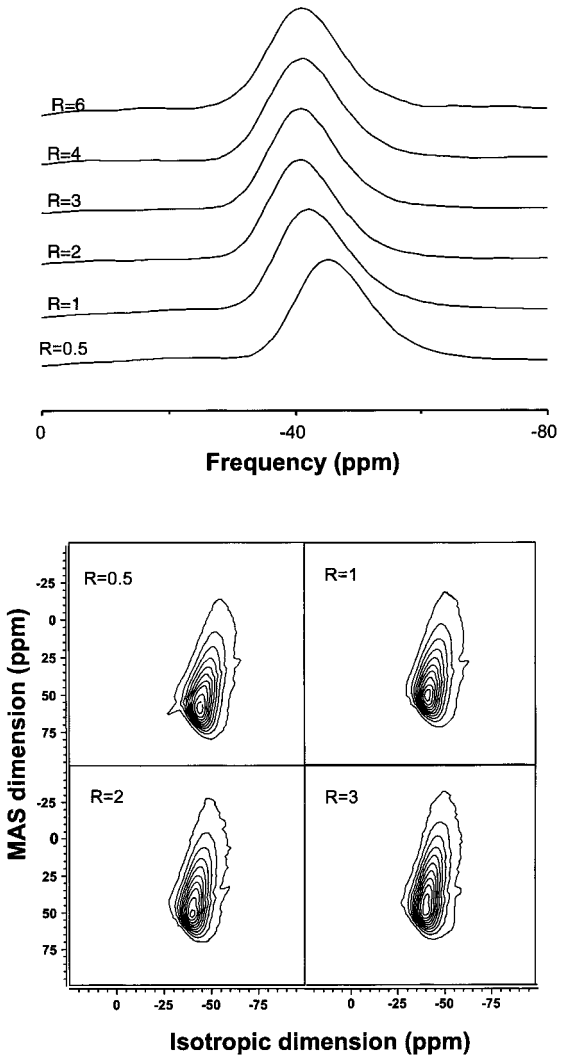

Figure 10. (a)^{27}Al 3QMAS NMR spectra of calcium aluminosilicate glasses with variable ratios (R) of Si/Al. Total projections in the isotropic dimension are shown above the 2-dimensional plot. 10 contour levels are drawn from 7 to 97% of maximum intensity.

sensitive to the structural configuration and chemical bonding around the atom of interest.[12,39−42] Therefore, variation of the parameters with composition can provide valuable information on the atomic configuration and degree of disorder.

δ_{iso}^{CS} values for Al sites in aluminosilicate glasses increase (δ_{3QMAS} decreases) with a decreasing number of Si next nearest neighbors, as illustrated by the fitting results for Na-aluminosilicate glasses (Figure 5).[8,12] This parameter has also been correlated with structural factors such as Al−O−Si bond angle.[30,43,44] The C_q for Al sites is dependent to a large degree on geometric factors such as deviations in bond-angle distribution and bond lengths from perfect tetrahedral or octahedral symmetry.[29] Q^4(0Si) and Q^4(4Si) sites are thus expected to have smaller C_q's than other species. The variation of peak position in ^{27}Al 3QMAS NMR spectra with respect to R in framework aluminosilicate glasses can thus be accounted by the variation of population of each Al environment [$Q^4(n\text{Si})$] with different C_q's.

In contrast to the relatively well-developed relationship between δ_{iso}^{CS} for ^{27}Al and intertetrahedral angle (T−O−T), definite correlations between δ_{iso}^{CS} for ^{17}O and atomic configurations and bonding in aluminosilicate glasses have not been firmly established.[19,45] δ_{iso}^{CS} may reflect variations of configuration not only at the nearest neighbor level but also to longer

range. Because of such complexities, it is not trivial to find definite interpretations for the trends observed here (i.e., that δ_{iso}^{CS} decreases with increasing R). However, this systematic trend with respect to R for all observed sites may suggest control by a single dominant factor, which can be ascribed to the increased shielding caused by decreased association with charge-balancing cations with increasing R. Similar trends have been reported in synthetic Na- and Na-, Ba− Y-type zeolites.[39,40]

A positive correlation between C_q, which is well correlated with the bond angle, and δ_{iso}^{CS} was reported for Si−O−Al sites in zeolite stilbite,[46] which may suggest that δ_{iso}^{CS} can also be correlated to intertetrahedral angle and local configurations caused by the introduction of charge-balancing cations into framework aluminosilicate glasses. Therefore, another possibility for the variation of δ_{iso}^{CS} may be the variation of average intertetrahedral angle and perhaps of ring topology with respect to R. The average ring size may increase with decreasing R. However, this trend was not observed in radial distribution functions obtained from X-ray scattering from Na-aluminosilicate glasses with varying R,[47] and a definite relationship between Si−O−Si angle and δ_{iso}^{CS} was not observed in crystalline coesite (SiO_2).[45]

The C_q for oxygen sites may be affected by several factors, such as bond angle, bond lengths, and number of nearby cations. With the increasing bond length between the charge-balancing cation and the bridging oxygen (BO), the C_q of the BO increases, and with the increasing number of charge-balancing cations near BO, the C_q decreases.[41,42,48] On the other hand, the range of variation of C_q with respect to Si−O−Si angle in coesite is less than 0.5 MHz, which may explain why our observed variation of C_q with respect to R is not prominent (Figure 8b).

As expected from the bond-valence concept and as can be seen from the differences of δ_{iso}^{CS} and C_q among the three types of oxygen sites reported here, more charge-balancing cations are associated with more negatively charged oxygen sites. Charge-balancing cations are not randomly distributed but are more selectively concentrated near Al−O−Al sites in lower silica glasses and near Al−O−Si sites in higher silica glasses. On the other hand, all of the oxygen sites interact with charge-balancing cations, to some degree, as shown in the results given here for Na-aluminosilicate glasses with varying R, including the systematic variation of δ_{iso}^{CS} with composition and the absence of abrupt changes in δ_{iso}^{CS} around $R = 1$ (Figure 8), implying that the clustering of framework cations maybe improbable.[15] The latter seems also to rule out the proposed possibility[49] of major change in the types of structural units from glasses with $R > 1$ to those with $R < 1$ and, thus, suggests that the types of coordination and atomic configurations of framework cations remain rather constant with R.

Effect of Cation Field Strength. As illustrated in Figure 8, δ_{iso}^{CS} values for oxygen sites increase with increasing cation field strength as has been suggested in Y-type zeolites. [39,40] The variations of P_q for Si−O−Al and Al−O−Al with respect to the cation field strength are not prominent considering the error range of this study. But the P_q for Al−O−Al does increase from Na to Li at $R = 1$ glasses and from Na to Ca for $R = 0.5$. A similar trend was reported for Si−O−Al sites in synthetic zeolites.[39]

The width of the distribution of δ_{iso}^{CS} values for Al−O−Al sites in Li− aluminosilicates is larger than that in Na-aluminosilicate glasses, which causes the increased peak overlap among oxygen sites with increasing cation field strength. As shown in our previous 3QMAS data,[15,19] the centers of gravity for Al−O−Al peaks in $R \leq 1$ glasses are distributed with slopes of about $-{}^{31}/_{17}$, which suggests that δ_{iso}^{CS} varies, but C_q's are nearly constant (assuming a constant C_q for spin-$^5/_2$ nuclei, $\delta_{MAS} = -{}^{31}/_{17}\delta_{3QMAS} + b$ where $b = {}^{27}/_{17}\delta_{iso}^{2Q} =$ constant). The number of configurations of Al−O−Al associated with Li^+ is larger than that for the Na^+ as manifested by an increased distribution of δ_{iso}^{CS} (Figure 7).

Higher field-strength cations may also lead to increased fractions of NBO. In La-and Y-aluminosilicate glasses,[6] the degree of disorder increases because 5- or 6- coordinated Al becomes abundant, producing correspondingly large fractions of NBO. Because Y^{3+} has a larger field strength than La^{3+}, the fractions of NBO and of 5- or 6- coordinated Al are even larger in Y-aluminosilicate glasses. (Unfortunately, the ^{17}O NMR peaks for BO in these glasses are not resolved into several components.) It is thus likely that the fractions of NBO and the accompanying degree of disorder in Na-aluminosilicate glasses are less than those found in Ca-aluminosilicate glasses, whose NBO fractions are less than 5%.[14] In charge-balanced aluminosilicate glasses, the formation of NBO can be associated with 3-coordinated oxygens called "triclusters".[50] However, direct evidence for triclusters has not yet been reported, despite indirect evidence, such as viscosity anomalies in Na-aluminosilicate liquids and the existence of NBO in charge-balanced Ca−aluminosilicate glasses.[14,18,51] In Na-aluminosilicates, known positions of NBO peaks overlap with Si−O−Al peaks making detection and quantification difficult. Furthermore, possible temperature effects on speciation must be taken into account in modeling melt properties above the glass transition temperature. In Ca-aluminosilicates, the existence of a few percent of NBO[14,21,51] suggests that some Q^3 species must be present, whose peak in ^{27}Al 3QMAS and ^{29}Si MAS spectra are overlapped with those for Q^4 species. In addition, there is also the possibility of AlO_5 species, as shown in the aluminosilicate glasses, with higher field strength cations.[6,52] On the other hand, most or all of the Al in Ca-, Li-, and Na-aluminosilicate glasses along charge-balance joins is 4-coordinated, with AlO_5 concentrations below typical detection limits of about 2−3%. Future studies with higher sensitivity may of course reveal this species at a lower detection limit. No evidence for Si in anything other than 4 coordination has been obtained from $R = 0.5$ to 6, consistent with standard models.[8]

The atomic structure and the ordering in such aluminosilicate glasses and melts with $R \leq 1$ seems to be less well understood. Recent ^{27}Al NMR data on $CaO-Al_2O_3$ glasses permitted estimation of Al coordination and NMR parameters.[53] Engelhardt et al. suggested the coexistence of equal amounts of $Q^4(4Al)$ and $Q^3(3Al)$ for the $Ca_2Al_2SiO_6$ glasses ($R = 0.5$), although this early study had difficulties imposed by low magnetic field and slow spinning speed.[54] According to recent energy-dispersive X-ray diffraction results, glasses with composition varying from SiO_2 to $CaAl_2Si_2O_8$ ($R = 1$) consist of defectless SiO_4 and AlO_4 units, whereas glasses with $R \leq 1$ are composed of defectless AlO_4 polyhedra and SiO_4 units with significant numbers of NBO with an average coordination of Si of less than four.[49] In a more traditional, ordered model, all of the tetrahedra are fully polymerized.[55] The existence of NBO in $R = 1$, 3, and 0.5 aluminosilicate glasses[14,19,51] suggests a relatively low concentration (less than about 10%) of Q^3 species in silicon (Q^3(mAl)) and Al environments (Q^3(nSi)), more consistent with standard models.[8,19]

Oxygen Site Populations, Degree of Al Avoidance, and Configurational Enthalpy. The degree of Si−Al disorder in aluminosilicate glasses obtained in this study provides important constraints on the thermodynamic properties of the correspond-

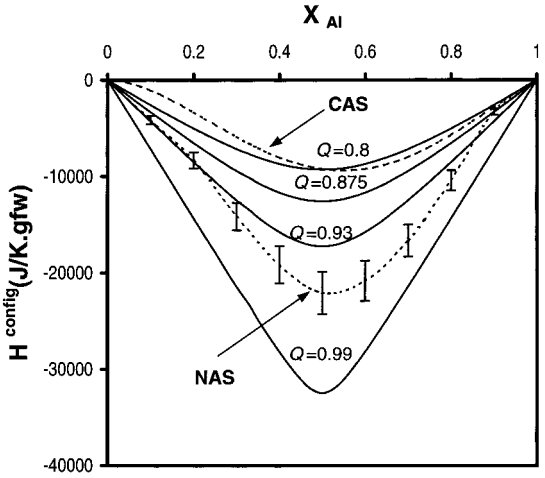

Figure 11. Calculated configurational enthalpy with respect to the degree of Al avoidance (Q). Solid lines show the ranges of configurational enthalpy calculated from the ranges of Q for Ca -and Na-aluminosilicate glasses. Dotted lines are the experimental enthalpies of mixing in the $SiO_2-Ca_{0.5}AlO_2$ (CAS) and the $SiO_2-NaAlO_2$ (NAS) system.[16]

ing liquids. In particular, the deviation from random mixing of framework cations in glasses can contribute to nonideality in both thermodynamic and transport properties.[56] The extent of disorder controls the configurational thermodynamic properties that stem from the chemical and structural arrangement of constituent atoms in the system. For example, configurational thermodynamic properties of the aluminosilicate glasses and liquids and the effect of cation field strength were recently calculated from the ^{29}Si MAS NMR data with a statistical thermodynamic model based on the quasi-chemical approximation.[8]

The systematic variations of the bridging oxygen site populations, with respect to R in Na- and Ca-aluminosilicate glasses that are reported here, were expected from ^{29}Si MAS NMR data, and can be used to obtain the degree of Al avoidance (Q). The populations of Al−O−Al and Si−O−Si in $LiAlSiO_4$ glass are greater than those in $NaAlSiO_4$ glasses, suggesting more disorder of framework cations in the former.[15] At 1050 K, approximate Q's for Na, Li, and Ca aluminosilicate glasses are 0.94, 0.9, and 0.85, respectively, which clearly manifests the effect of the cation field strength on the extent of disorder. This trend affects the configurational thermodynamic properties and, thus, the transport properties of aluminosilicate melts (i.e., an increase in the field strength of charge-balancing cation leads to an increase in the configurational entropy, a decrease in viscosity, and an increase in the fragility (the rapidity of decrease in viscosity above the glass transition)).[57] The configurational entropy of $CaAl_2Si_2O_8$, $LiAlSiO_4$, and $NaAlSiO_4$ glasses calculated from oxygen site populations at 1050 K, assuming the random mixing between oxygen pairs, are 6.53(±0.4), 5.94(±0.15), and 5.2(±0.15) J/K·gfw, respectively.[15] The formation of more Al−O−Al and Si−O−Al with decreasing R and with increasing cation field strength in charge-balanced aluminosilicates leads to the increase in the width of the bond angle distribution function as obtained from a molecular dynamics simulation.[58]

The enthalpies of mixing, calculated from the degree of disorder based on quasi-chemical approximation[8] and thus considering only the relative energy difference and site population among Al−O−Al, Si−O−Si, and Al−O−Si in Ca- and Na-aluminosilicate glasses, are compared with the data obtained from solution calorimetry (Figure 11).[16] The enthalpy of mixing in the $SiO_2-Ca_{0.5}AlO_2$ system was expressed with a second-order Ridlich−Kister equation[16] that is consistent with the configurational enthalpy calculated from the degree of order in calcium aluminosilicate glasses at 985 K.[8] As for the sodium aluminosilicate glasses, the experimental enthalpy of mixing can be predicted from the calculated ranges of configurational enthalpy. The thermodynamic excess properties of aluminosilicate glasses and melts can be calculated from the short range ordering scheme obtained from NMR spectroscopy mainly because short-range interaction among tetrahedral cations is one of the major contributions to the total potential energy in the glasses.

Conclusions

The degree of Al avoidance in aluminosilicate glasses can be estimated from the site populations obtained from ^{27}Al and ^{17}O 3QMAS NMR and adjusted for the dependence of 3QMAS efficiency on C_q. In particular, ^{17}O 3QMAS NMR provides clear and direct data regarding the extent of disorder when calibrated as described here. The extent of deviation from Al avoidance, and thus the configurational entropy, increases from Na- to Ca-aluminosilicate glasses. This trend is consistent with the prediction that with increasing cation field strength, the degree of disorder increases. The Al−O−Al site population is also proportional to the cation field strength. With increasing cation field strength, the disorder in the framework cation distribution, and therefore possible topological arrangements and Al−O−Al site populations, increase. The concentration of NBO may also increase with increasing cation field strength.

From the detailed analysis of 3QMAS spectra of quadrupolar nuclei, we can obtain information on the atomic structure of aluminosilicate glasses with varying silicon-to-aluminum ratio (R) and varying cation field strength through the variation of structurally relevant NMR parameters. The framework cations are dominantly 4-coordinated. Not only can the short-range order be obtained, but also, some aspects of the medium-range order of the framework cation distribution can be inferred. The proportions of aluminum sites with 4 Al next nearest neighbor is negligible in $R = 1$ Na- and Ca-aluminosilicates. Therefore, the local clustering of Al is improbable. Charge-balancing cations are distributed more closely to oxygen linkages with higher local charge, such as NBO and Al−O−Al sites. On the other hand, all of the oxygen sites interact with those cations to some degree, and this interaction varies systematically with R, suggesting no discontinuity in the effect of composition on local framework connectivity.

Acknowledgment. This project was supported by NSF Grant No. EAR9803953 and a Stanford Graduate Fellowship. We thank Dr. P. Zhao and Dr. S. Kroeker for helpful discussions and two anonymous reviewers for helpful comments on the original manuscript.

References and Notes

(1) Riebling, E. F. *J. Chem. Phys.* **1966**, *44*, 2857−2865.
(2) Mysen, B. O.; Virgo, D.; Seifert, F. A. *Rev. Geophys. Space Phys.* **1982**, *20*, 353−383.
(3) Risbud, S. H.; Kirkpatrick, R. J.; Taglialavore, A. P.; Montez, B. *J. Am. Ceram. Soc.* **1987**, *70*, C10−C12.
(4) Zirl, D. M.; Garofalini, S. H. *J. Am. Ceram. Soc.* **1990**, *73*, 2848−2856.
(5) Jewell, J. M.; Shaw, C. M.; Shelby, J. E. *J. Non-Cryst. Solids.* **1993**, *152*, 32−41.
(6) Schaller, T.; Stebbins, J. F. *J. Phys. Chem. B* **1998**, *102*, 10 690−10 697.
(7) Xu, Z.; Maekawa, H.; Oglesby, J. V.; Stebbins, J. F. *J. Am. Chem. Soc.* **1998**, *120*, 9894−9901.

(8) Lee, S. K.; Stebbins, J. F. *Am. Mineral.* **1999**, *84*, 937−945.
(9) Zeng, Q.; Nekvasil, H.; Grey, C. P. *J. Phys. Chem. B* **1999**, *103*, 7406−7415.
(10) Xue, X.; Kanzaki, M. *J. Phys. Chem. B* **1999**, *103*, 10 816−10 830.
(11) Murdoch, J. B.; Stebbins, J. F.; Carmichael, I. S. E. *Am. Mineral.* **1985**, *70*, 332−343.
(12) Engelhardt, G.; Michel, D. *High-Resolution Solid-State NMR of Silicates and Zeolites*; Wiley: New York, 1987.
(13) Oestrike, R.; Yang, W. H.; Kirkpatrick, R.; Hervig, R. L.; Navrotsky, A.; Montez, B. *Geochim. Cosmochim. Acta* **1987**, *51*, 2199−2209.
(14) Stebbins, J. F.; Xu, Z. *Nature* **1997**, *390*, 60−62.
(15) Lee, S. K.; Stebbins, J. F. *J. Non-Cryst. Solids.* **2000**, *270*, 260−264.
(16) Navrotsky, A.; Peraudeau; McMillan, P.; Coutures, J. P. *Geochim. Cosmochim. Acta* **1982**, *46*, 2039−2047.
(17) Richet, P. *Geochim. Cosmochim. Acta* **1984**, *48*, 471−483.
(18) Toplis, M. J.; Dingwell, D. B.; Hess, K.; Lency, T. *Am. Mineral.* **1997**, *82*, 979−990.
(19) Stebbins, J. F.; Lee, S. K.; Oglesby, J. V. *Am. Mineral.* **1999**, *84*, 983−986.
(20) Dirken, P. J.; Kohn, S. C.; Smith, M. E.; Vaneck, E. R. H. *Chem. Phys. Lett.* **1997**, *266*, 568−574.
(21) Stebbins, J. F.; Zhao, P.; Lee, S. K.; Cheng, X. *Am. Mineral.* **1999**, *84*, 1680−1684.
(22) Medek, A.; Harwood, J. S.; Frydman, L. *J. Am. Chem. Soc.* **1995**, *117*, 12779.
(23) Wu, G.; Rovnyank, D.; Sun, B.; Griffin, R. G. *Chem. Phys. Lett.* **1996**, *249*, 210−217.
(24) Wang, S. H.; Xu, Z.; Baltisberger, J. H.; Bull, L. M.; Stebbins, J. F.; Pines, A. *Solid State NMR* **1997**, *8*, 1−16.
(25) Ding, S. W.; McDowell, C. A. *Chem. Phys. Lett.* **1999**, *307*, 215−219.
(26) Vega, S. *J. Chem. Phys.* **1977**, *68*, 5518−5527.
(27) Beall, G. H. Industrial applications of silica. In *Silica*; Heaney, P. J., Prewit, C. W., Eds.; Mineralogical Society of America: Washington, D. C., 1994; Vol. 29, pp 469−505.
(28) Lee, K. H.; Hirschfeld, D. A.; Brown, J. J. *J. Am. Ceram. Soc.* **1996**, *79*, 597−602.
(29) Ghose, S.; Tsang, T. *Am. Mineral.* **1973**, *58*, 748−755.
(30) Baltisberger, J. H.; Xu, Z.; Stebbins, J. F.; Wang, S.; Pines, A. *J. Am. Chem. Soc.* **1996**, *118*, 7209−7214.
(31) Vega, S.; Noar, Y. *J. Chem. Phys.* **1981**, *75*, 75−86.
(32) Amoureux, J. P.; Fernandez, C.; Frydman, L. *Chem. Phys. Lett.* **1996**, *259*, 347−355.
(33) Vega, A. J. *J. Magn. Reson.* **1992**, *96*, 50−68.
(34) Alemany, L. B.; Steuernagel, S.; Amoureux, J. P.; Callender, R. L.; Barron, A. R. *Solid State NMR* **1999**, *14*, 1−18.
(35) Jäger, C.; Kunath, G.; Losso, P.; Scheler, G. *Sol. State Magn. Reson.* **1993**, *2*, 73−82.
(36) Skibsted, J.; Henderson, E.; Jakobsen, H. J. *Inorg. Chem.* **1993**, *32*, 1013−1027.
(37) Yang, W. H.; Kirkpatrick, R. J.; Henderson, D. M. *Am. Mineral.* **1986**, *71*, 712−726.
(38) Johnson, R. T.; Biefeld, R. M.; Knotek, M. L.; Morosin, B. *J. Electrochem. Soc.* **1976**, *123*, 680−687.
(39) Timken, H. K. C.; Janes, N.; Turner, G. L.; Lambert, S. L.; Welsh, L. B.; Oldfield, E. *J. Am. Chem. Soc.* **1986**, *108*, 7236−7241.
(40) Timken, H. K.; Turner, G. L.; Gilson, J. P.; Welsh, L. B.; Oldfield, E. *J. Am. Chem. Soc.* **1986**, *108*, 7231−7235.
(41) Vermillion, K. E.; Florian, P.; Grandinetti, P. J. *J. Chem. Phys.* **1998**, *108*, 7274−7285.
(42) Clark, T. M.; Grandinetti, J. *Abstract Am. Chem. Soc.* **1999**.
(43) Phillips, B. L.; Kirkpatrick, R. J.; Carpenter, M. A. *Am. Mineral.* **1992**, *77*, 484−495.
(44) Lippmaa, E.; Samoson, A.; Mägi, M. *J. Am. Chem. Soc.* **1986**, *108*, 1730−1735.
(45) Grandinetti, P. J.; Baltisberger, J. H.; Farnan, I.; Stebbins, J. F.; Werner, U.; Pines, A. *J. Phys. Chem.* **1995**, *99*, 12 341−12 348.
(46) Xu, Z.; Stebbins, J. F. *Solid State NMR* **1998**, *11*, 243−251.
(47) Taylor, M.; Brown, G. E., Jr. *Geochim. Cosmochim. Acta* **1979**, *43*, 1467−1473.
(48) Maekawa, H.; Florian, P.; Massiot, D.; Kiyono, H.; Nakamura, M. *J. Phys. Chem.* **1996**, *100*, 5525−5532.
(49) Petkov, V.; Gerber, T.; Himmel, B. *Phys. Rev. B.* **1998**, *58*, 11 982−11 989.
(50) Lacy, E. D. *Phys. Chem. Glasses* **1963**, *4*, 234−238.
(51) Stebbins, J. F.; Oglesby, J. V.; Lee, S. K. *Chem. Geol.* **2000**, in press.
(52) McMillan, P. F.; Kirkpatrick, R. J. *Am. Mineral.* **1992**, *77*, 898−900.
(53) McMillan, P. F.; Petuskey, W. T.; Cote, B.; Massiot, D.; Landron, C.; Coutures, J. P. *J. Non-Cryst. Solids.* **1996**, *195*, 261−271.
(54) Sato, R. K.; Mcmillan, P. F.; Dennison, P.; Dupree, R. *Phys. Chem. Glasses* **1991**, *32*, 149−156.
(55) Kirkpatrick, R. J.; Dunn, T.; Schramm, S.; Smith, K. A.; Oestrike, R.; Turner, G. Magic-Angle Sample-Spinning Nuclear Magnetic Resonance Spectroscopy of Silicate Glasses: a Review. In *Structure and Bonding in Noncrystalline Solids*; Walrafen, G. E., Revesz, A. G., Eds.; Plenum Press: New York, 1986; pp 302−327.
(56) Tomozawa, M. *Solid State Ionics* **1998**, *105*, 249−255.
(57) Angell, C. A. *Science* **1995**, *267*, 1924−1935.
(58) Scamehorn, C. A.; Angell, C. A. *Geochim. Cosmochim. Acta* **1991**, *55*, 721−730.